Analytica Chimica Acta 1369 (2025) 344366

Contents lists available at ScienceDirect

Analytica Chimica Acta

journal homepage: www.elsevier.com/locate/aca

Early insulin fibril detection: Insulin fibril research and TR structural transition detection with FRET-Probe

Morteza Malakoutikhah [a,b], Laura Kauppi [a], Kalle Mäntylä [a], Harri Härmä [a], Kari Kopra [a,*]

[a] Department of Chemistry, University of Turku, Henrikinkatu 2, 20500, Turku, Finland
[b] Alimetrics Research Ltd., Koskelontie 19B, 02920, Espoo, Finland

HIGHLIGHTS

- The FRET-Probe enables early and sensitive detection of insulin fibril formation.
- Recombinant and commercial insulins can be studied using wide concentration range.
- Developed technique can monitor structural insulin hexamer TR transition events.
- Conversion from the visible hexamer T-state to R-state can be monitored in real-time.
- External luminescent probe provides a method for insulin engineering and formulation.

GRAPHICAL ABSTRACT

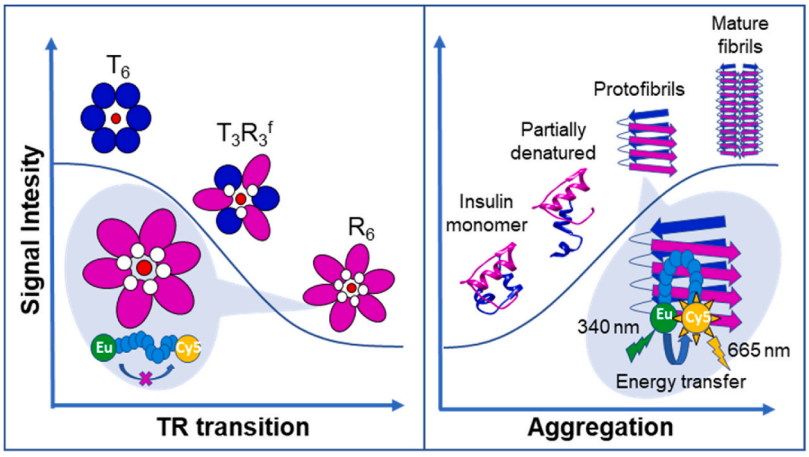

ARTICLE INFO

Handling Editor: Professor Chuck Henry

Keywords:
Insulin
Fibers
FRET-Probe
Aggregation
Thioflavine T (ThT)
TR transition

ABSTRACT

Background: The detection of amyloid fibrils is critical in production, storage and therapeutic use of insulin due to impact on efficacy and potential cytotoxicity after injection. Monitoring insulin aggregation, particularly at early stages, offers a valuable insight to aid the design of stable and effective insulin analogs, and addressing challenges in diabetes management. Despite numerous methods and probes developed this far, the detection of insulin fibers at nanomolar concentrations has remained a challenge. Moreover, as rapid-acting or slow-acting engineered insulin analogs are constantly developed, simple and sensitive methodologies also for monitoring structural transition of hexameric TR insulin forms are needed.
Results: To address limitations in methodologies for insulin research, we developed an intramolecular Förster Resonance Energy Transfer (FRET) based peptide-probe, named as the FRET-Probe, for the detection of insulin fibers and hexamer TR transition changes at nanomolar concentrations. Using a comprehensive panel of insulin concentrations and therapeutically available insulin formulations, we highlight the sensitivity of the FRET-Probe

* Corresponding author. Department of Chemistry, University of Turku, Henrikinkatu 2, 20500, Turku, Finland.
E-mail address: kari.kopra@utu.fi (K. Kopra).

https://doi.org/10.1016/j.aca.2025.344366
Received 1 April 2025; Received in revised form 23 June 2025; Accepted 24 June 2025
Available online 25 June 2025

in insulin fibril detection at early stages. In a comparative study with thioflavin T (ThT), we demonstrated 15-fold improved sensitivity of the FRET-Probe, and its ability for early insulin fiber detection. In addition, we demonstrate the ability of the FRET-Probe to differentiate between insulin hexameric forms (T_6, T_3R_3, and R_6), in the presence of anionic ligands and phenol derivatives. Thus, the FRET-Probe provides an unprecedented tool for characterizing structural dynamics using a luminescent external probe.

Significance: The FRET-Probe provides a simple and sensitive method for insulin fibril detection, enabling significantly improved detection of especially early insulin aggregation events, in comparison to ThT. The FRET-Probe also provides valuable insights into insulin analog stability and function, enabling insulin hexamer conformational measurements in real-time. The FRET-Probe can give comprehensive perspective on insulin behavior in varying conditions, thus supporting the insulin engineering and formulation processes.

1. Introduction

Insulin is a small protein composed of two polypeptide chains (A and B) linked by two disulfide bonds. In mammalians, it is produced by the β-cells of the pancreas, where it is stored as a hexamer stabilized by two zinc ions. When entering the bloodstream, it dissociates into active monomers that bind to insulin receptors [1]. Insulin is essential for regulating blood sugar levels and treating diabetes. Diabetes is a growing global health concern, with its prevalence increasing due to population growth, aging, and rising rates of inactivity and obesity. Type 1 diabetes results from an autoimmune destruction of the β-cells while type 2 diabetes is characterized by β-cell dysfunction and insulin resistance [2,3]. The prevalence of diabetes was estimated to have risen from 198 million in 1990 to notable 828 million in 2022 [4].

Insulin stability is influenced by its structural form, as insulin hexamer is more stable than the monomer against degradation and denaturation [5,6]. Insulin hexamer exhibits equilibrium among three forms, T_6, $T_3R_3^f$ and R_6. The addition of zinc to insulin promotes the formation of T_6 hexamers at sufficient insulin concentrations, while chaotropic anions and phenolic compounds shift the hexameric equilibrium toward more stable $T_3R_3^f$ and R_6 forms [5,6]. The "relaxed" R_6 insulin differs from the "tense" T_6 insulin by extending the helical structure of monomers to include the first eight amino acids on the B-chain. In the $T_3R_3^f$ insulin, consisting of dimers in both T- and R-state, the R monomer adopts a "frayed" conformation, where the three first amino acids of the B-chain are in an extended state [7]. The additives promoting R_6 hexamer formation are usually added to therapeutic formulations to enhance insulin stability [8].

Different patients have varying needs for insulin, and thus novel insulin analogs with altered amino acid structure have been developed. Rapid-acting analogs, such as aspart and glulisine, accelerate hexamer dissociation to increase absorption rates. These engineered analogs have only minor changes in their sequences, for example, in aspart single proline (B28) is displaced with aspartic acid, while in glulisine, asparagine (B3) and lysine (B29) are substituted with lysine and glutamic acid, respectively [9,10]. Even though ultrarapid insulins have also been developed [11], slow-acting analogs like glargine have their own market to achieve extended release. In glargine, asparagine (A21) is replaced with glycine, and two arginine residues are added to the B-chain *C*-terminus. This leads to a shift in the isoelectric point, enhancing solubility in acidic solutions (formulated at pH 4), but inducing precipitation upon injection into neutral pH. This aggregate dissolves slowly to provide up to 24 h of insulin release [12]. However, often aggregation is an unwanted phenomenon. It occurs during insulin production, storage and upon subcutaneous injection, causing amyloid fibers to form [13,14]. Aggregation is promoted by conditions such as pH shifts [15], high temperatures [16], agitation [17], contact with hydrophobic surfaces [18], and the aggregation tendency is insulin analog specific [19]. In disfavoring environment, insulin monomers may partially unfold, forming β-sheet-rich protofilament cores that extend into amyloid fibrils [20–22]. These fibrils reduce insulin bioavailability and can trigger immune responses or cytotoxic effects [13,14].

Given the clinical and pharmaceutical implications, early and low-concentration detection of insulin fibers and conformation is critical. Numerous methods, discussed in more detail in Table S1, including Fourier transform infrared spectroscopy (FTIR) [23], circular dichroism (CD) [22], transmission electron microscopy (TEM) [22], cryo-electron microscopy (cryo-EM) [20,21] light scattering [24], and capillary electrophoresis (CE) [25], have been employed to monitor insulin aggregation. FTIR and CD analyze conformational changes associated with fibril formation. CD can be used not only for aggregates, but also for TR transition monitoring [26]. Light scattering detects the size, and can be mainly used for large aggregates, but lacks sensitivity to early intermediates and small concentrations. CE effectively separates insulin monomers from oligomers, which are present in early-state aggregation, but has relatively hard implementation.

Fluorescent probes, particularly the gold standard thioflavin T (ThT), are commonly used to study insulin fibrillation, due to their simple protocols. ThT binds to β-sheet-rich amyloid fibrils, generating fluorescence signals to quantify mature fibrils [27]. However, ThT does not enable the detection of early-stage oligomers and has low sensitivity. Other probes, such as 8-Anilinonaphthalene-1-sulfonic acid (ANS) [28] and Nile red [29], detect changes in hydrophobicity during aggregation but lack specificity for fibrillar structures, typical to insulin aggregates. Unfortunately, insulin structural changes prior aggregation is not detected with these fluorescent probes.

To our knowledge, none of the existing methods have demonstrated the detection of insulin fibers at nanomolar concentration. Furthermore, their ability to differentiate early structural transitions, such as β-sheet formation or changes in aggregate morphology is often constrained by their detection limits. Earlier, we have introduced an intramolecular FRET-Probe [30], as a tool to monitor protein stability. This dual-labeled negatively charged peptide-probe changes its structure upon binding to its target, monitored as increased time-resolved Förster resonance energy transfer (TR-FRET) signal. Here, we utilized this tool to monitor insulin aggregation under acidic and neutral buffer conditions, by detecting insulin fibers at nanomolar sensitivity. The method offers potential to resolve early-stage aggregation, in significantly improved fashion compared to ThT. In addition, we demonstrate the FRET-Probes ability to distinguish different insulin hexameric forms, providing a valuable insight into insulin analog development, by monitoring insulin TR transition changes in the presence of additives.

2. Experimental section

2.1. Materials and methods

Detailed list of materials and instrumentation, and protocols related to preparation of the insulin, β-amyloid peptide 1–42 ($A\beta_{42}$), and islet amyloid polypeptide (IAPP) fibrils, luminescence decay measurements, TEM imaging, and data analysis are presented in Supplementary Material. All presented assays were performed in triplicates unless otherwise indicated.

2.2. Fibrillation detection in acidic pH

The FRET-Probe (0.03–7.6 nM) and ThT (0.2–200 μM) concentration was optimized using insulin fibers (50 μM) produced in HCl (pH 1.8),

100 mM NaCl. Aggregated or non-aggregated insulin (2 μL) was added to a 384-well plate, followed by addition (20 μL) of the FRET-Probe in 10 mM Tris-HCl (pH 7.5), 0.01 % Triton X-100 or ThT in 50 mM phosphate buffer (pH 7.4). After 5 min incubation, TR-FRET (FRET-Probe) and ThT fluorescence signals were measured. Fibrillation process was monitored using opposite addition order. For $A\beta_{42}$ and IAPP assays, the FRET-Probe (1 nM) or ThT (10 μM) was first added in 65 μL and 100 μL volume, respectively. Thereafter, 2 μL (FRET-Probe) or 5 μL (ThT) fiber samples were added, respectively. For insulin, 1 nM FRET-Probe or 3 μM ThT was used in 20 μL volume, followed the addition of 2 μL fiber sample. TR-FRET and ThT fluorescence signals were measured as previously. The same protocol was used for insulin titration (0.004–18.2 μM in a final 22 μL volume), performed by diluting either the 200 μM (28 h at 60 °C) or 50 μM insulin fibers (6 or 8 h at 60 °C). FRET-Probe and ThT concentrations are given in final 22 μL volume, and the insulin concentration is given in a fibril formation reaction, unless otherwise indicated, which is diluted 11-fold in the well.

2.3. Fibrillation detection in neutral pH

The FRET-Probe (0.06–7.6 nM) and ThT (0.5–50 μM) concentrations were optimized using insulin fibers (50 μM) produced in 20 mM HEPES (pH 7.5) supplemented with 100 mM NaCl. To study the effects of concentration, fiber production was conducted without the addition of NaCl. Aggregated or non-aggregated insulin (2 μL) was added to a 384-well plate, followed by addition (20 μL) of the FRET-Probe in 7.7 mM Na_2HPO_4, 6.1 mM citric acid (pH 4), 0.01 % Triton X-100 or ThT in PBS (pH 7.4). TR-FRET and ThT fluorescence signals were measured as previously after 5 min incubation. As in the case of acidic pH, all other assays were performed with the opposite addition order, 20 μL detection (0.5 nM FRET-Probe or 6.3 μM ThT) and 2 μL of insulin sample. Also, the therapeutic insulins (~600 μM) were using this protocol.

2.4. Insulin TR transition monitoring

Insulin hexamer conformation determination assays were performed only with the FRET-Probe (1 nM). In the resorcinol titration (0.78–200 mM), 20 μL of the FRET-Probe was added in 20 mM HEPES (pH 7.5), 0.01 % Triton X-100 solution. Thereafter, 2 μL of the 600 μM insulin samples (54.5 μM in well) with 150 μM $ZnCl_2$, in the absence or presence of 50 mM KSCN and 200 mM NaCl, and varying concentration of resorcinol were added in phosphate buffer (7 mM, pH 7.4). TR-FRET signals were monitored after 5 min incubation. Measurements were conducted using a black 384-well microtiter plate (4titude, Surrey, U. K.). TR transition measurements were performed stepwise, in which the individual components were added to the same wells containing the FRET-Probe (1 nM) in 20 μL. The addition order was; 1. insulin (30 μM), 2. $Zn(ClO_4)_2$ (12 μM), 3. KSCN (5 mM), and 4. resorcinol (5 mM), and the TR-FRET signal was monitored at every step after 10 min incubation using black 384-well microtiter plate (Corning, Kennebunk, MA, USA). All additions were made in H_2O (1 μL), and the concentration for insulin and $Zn(ClO_4)_2$ is given in 22 μL, and for KSCN and resorcinol in 23 and 24 μL, respectively.

3. Results and discussion

3.1. FRET-probe distinguishes native and aggregated insulin

We have previously introduced the FRET-Probe consisting a luminescent europium (Eu^{3+}) chelate and a cyanine 5 (Cy5) dye acceptor, coupled to the *N*- and *C*-termini of a negatively charged peptide, respectively, illustrated in Fig. 1A [30]. The FRET-Probe was developed to study protein thermal and chemical stability, and it has been shown to detect structural changes in proteins, monitored as TR-FRET signal. This is due to distance dependent shift between the donor and acceptor labels upon the FRET-Probe conformational change. This ability allows the monitoring of insulin structure and aggregation, which was validated using ThT, the gold standard assay, as our main reference method (Fig. 1B).

Insulin is known to aggregate for example at low pH, increased temperature and agitation, also leading to aggregate variations [15–18, 31,32]. To prove the FRET-Probe ability to detect insulin fibrils, we first conducted assays with native insulin and insulin fibrils formed at low pH (HCl pH 1.8 + NaCl 100 mM) by measuring FRET-Probe emission spectra using 340 nm excitation wavelength. Under these conditions, no TR-FRET signal at the expected Cy5 maximum (~670 nm) was detected in buffer or in the presence of native insulin. However, 70-fold increase in TR-FRET emission, maximum at 672 nm, was detected upon addition of insulin fibrils (Fig. S1A). To confirm that the formed aggregate is amyloid type, a similar experiment was conducted using ThT as a control (Fig. S1B). ThT results as an increase in the emission at 494 nm were consistent with the FRET-Probe signal change, while the buffer or native insulin showed no increase in ThT emission (Fig. S1B). To better understand the molecular basis of the TR-FRET signal observed with the FRET-Probe, we investigated the luminescence decays of the FRET-Probe in the presence of insulin incubated 0–8 h at low pH (HCl pH 1.8 + 100 mM NaCl) (Fig. S2). The data show a clear increase in monitored lifetime in a relation to insulin aggregation progresses. This indicates that structural changes within the probe are occurring upon interaction with insulin fibers and therefore increasing the monitored TR-FRET signal.

After showing the functionality with insulin, we further tested the FRET-Probe with $A\beta_{42}$ and IAPP to provide preliminary evidence of the wider applicability of this probe across different amyloid fibrils (Fig. S3). $A\beta_{42}$ and IAPP (20 μM) were incubated in 10 mM HCl (pH 2) at 37 °C, and samples were collected at various time points (0–72 h for

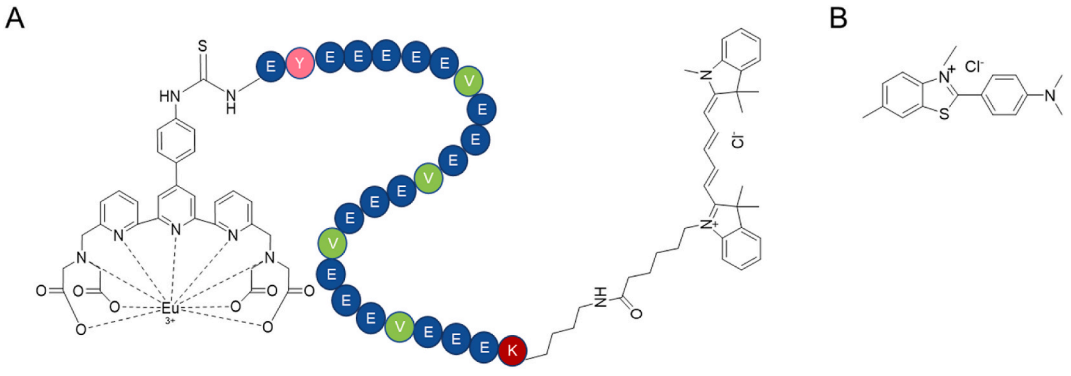

Fig. 1. Chemical structures of the FRET-Probe and thioflavin T (ThT). **(A)** Structure of the FRET-Probe comprises *N*-terminal luminescent Eu^{3+}-chelate, acting as a donor, and organic Cy5 acceptor conjugated at *C*-termini of a negatively charged glutamic acid-rich peptide. (**B**) The structure of ThT contains a benzylamine and a benzothiazole ring connected through a carbon-carbon bond, and the rotational changes are detected as changes in fluorescence signal.

$A\beta_{42}$; 0–75 h for IAPP). These samples were then analyzed using both the FRET-Probe and ThT. With both methods, $A\beta_{42}$ was clearly detected after 23 h of incubation, but with the FRET-Probe, already after 7.5 h, which was the earliest time point used (Fig. S3A). In case of IAPP, fibril formation was clearly delayed under the same acidic conditions used for $A\beta_{42}$ [33]. This can explain the minimal increase in ThT fluorescence over time, as the FRET-Probe started to increase already after 48 h, providing a clear ~5-fold TR-FRET signal increase after 75 h (Fig. S3B). This indicated that the FRET-Probe has improved sensitivity over ThT in case of both $A\beta_{42}$ and IAPP. Additionally, the use of increased concentration of $A\beta_{42}$ (20–100 μM) did not improve the ThT-based detection at early time points, even the obtained fluorescence signal was increased (Fig. S3C). The fibril formation was further confirmed with TEM images (Fig. S3D), but as insulin was the main target in our study, assays with $A\beta_{42}$ and IAPP were not further continued. However, already these results highlight the FRET-Probe's broader applicability for detecting diverse amyloid fibrils.

3.2. High sensitivity detection of insulin aggregates

Initial experiments demonstrated that both the FRET-Probe and ThT can detect insulin fibrils at high concentration. To enable more sensitive detection, a careful optimization of assay conditions was required. The optimal probe concentration is critical in balancing between sensitivity and specificity. Previously, a wide range of ThT concentrations (typically 1–100 μM) [31,32,34,35] have been employed for the detection of insulin fibrils, and notably, there has been a lack of systematic evaluation to determine the optimal concentration of ThT. This is especially important, as it is known that the maximal ThT signal depends mostly on the ThT concentration rather than the fibril to ThT ratio [36].

We first evaluated the effect of ThT concentration on the signal-to-background (S/B) ratio in the detection of 50 μM differently aged insulin fibrils, and performed the same measurements with the FRET-Probe. For this study, insulin was incubated for 8-, 24- or 70 h using HCl (pH 1.8) supplemented with 100 mM NaCl. The results indicate that the functionality of the FRET-Probe is not dependent on the fibril age. In all cases the highest S/B ratios were observed using 1 nM FRET-Probe or 3 μM ThT concentrations (Fig. S4). These optimized concentrations were used for the rest of the studies. Notably, the 1 nM FRET-Probe demonstrated consistent fibril detection, as the S/B ratios were equal (162–164) for the differently aged samples. This consistency across insulin fibril detection suggests that the interaction between the FRET-Probe and insulin fibrils remains relatively stable independently of fibril age, and thus its form. The data also indicates that, the assay reached the signal saturation in all cases. In contrast, ThT showed greater variability in S/B ratios across fibril ages. With 3 μM ThT concentration, S/B values detected were 17, 99, and 139 for the 8, 24, and 70 h samples, respectively. Thus, the ThT ability to monitor fibrils at earlier states is significantly lower than with the FRET-Probe.

Since the FRET-Probe consistently demonstrated fibril detection over the given times, we next evaluated concentration and time dependent insulin aggregation. We prepared solutions with four different insulin concentrations (1, 5, 25 and 50 μM) in acidic conditions, and subjected these to 48 h incubation at 60 °C. Samples were collected at designated time intervals, and thereafter analyzed using the FRET-Probe and ThT in their optimal concentrations. The results unveiled characteristic sigmoidal curves for insulin aggregation, featuring a lag phase, exponential growth, and eventual plateau (Fig. 2A). The expected trend emerged, where the higher insulin concentrations led to a shorter lag time, indicating faster insulin aggregation [34,37,38]. The FRET-Probe demonstrated a shorter lag time than the ThT for all samples. proved by its higher sensitivity to detect formed fibers. Furthermore, the FRET-Probe exhibited substantially higher S/B ratios in comparison to ThT across all concentrations. Especially at the lowest insulin concentration (1 μM), the FRET-Probe showed its high capability to detect the formed fibers, while ThT struggled to detect fibrils even after 48 h of incubation (Fig. 2B). The FRET-Probe detected insulin fibrils after 13 h, ultimately resulting in an impressive S/B ratio of 5 after 48 h.

As typical ThT insulin assays are performed at high concentrations, we continued our investigation by performing experiments using 200

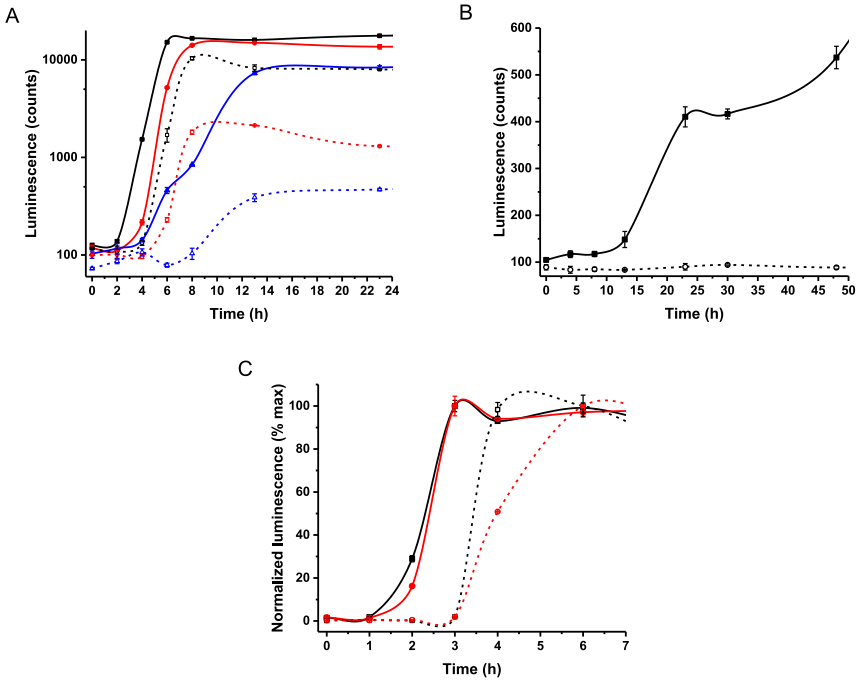

Fig. 2. Insulin aggregation detection with the FRET-Probe (1 nM, solid line) and ThT (3 μM, dashed line) at varying insulin concentrations. Insulin fibers were formed at (**A**) 5 (blue), 25 (red) and 50 μM (black), (**B**) 1 μM and (**C**) 200 (red) and 400 μM (black) insulin in HCl pH 1.8 containing 100 mM NaCl at 60 °C. Data are presented as the mean ± SD (n = 3). (For interpretation of the references to colour in this figure legend, the reader is referred to the Web version of this article.)

and 400 μM insulin (Fig. 2C). Also under these conditions, the FRET-Probe consistently exhibited a shorter lag time in comparison to ThT. This persistent pattern underscores sensitivity of the FRET-Probe in over ThT, but also greater dynamics over a wide range of insulin concentrations. Interestingly, the increase in insulin concentration from 200 to 400 μM, had only a minor effect on insulin detectability in both assays.

3.3. Fibril detection proved via TEM images

To verify that the increase in the FRET-Probe signal is due to fiber formation, TEM images were taken from 25 μM insulin samples incubated in HCl (pH 1.8) for 6- and 23 h (Fig. S5). Conditions were selected based on the results observed earlier (Fig. 2A), where the FRET-Probe but not ThT (6 h) reached the signal saturation, and later the point in which the aggregation was well saturated with both methods (23 h). TEM images confirmed the presence of insulin fibers already after 6 h of incubation, with a notable increase in fibril abundance after 23 h. These findings give a strong confirmation that the saturation of FRET-Probe signal at 6 h samples (Fig. 2A), indeed is due to fiber formation. Only a modest 2-fold increase in ThT signal was measured in these conditions (Fig. 2A). The TEM validation not only strengthens the evidence for the FRET-Probe capacity to measure insulin fibers but also emphasizes its ability for early-stage detection. Interestingly, insulin fibrils are shorter in comparison to what was seen with $A\beta_{42}$ (Fig. S3D and S5), but the effect of fibril morphology for their detectability with either ThT or the FRET-Probe was not further studied.

3.4. Detecting non-mature aggregates

After confirming the FRET-Probe detection of insulin fibers, we further studied to understand FRET-Probe capacity to detect non-maturated fibrils. First, fully aggregated insulin was first prepared using 200 μM insulin solution at 60 °C for 28 h and thereafter, the solution was diluted and titrated from 0.018 to 18.2 μM with the FRET-Probe and ThT. Both methods show linear correlation and the signal increase was monitored upon fiber concentration increase (Fig. 3A). As expected, the FRET-Probe reached saturation at lower concentration in comparison to ThT. However, in this assay setup, there is no clear difference between the FRET-Probe and ThT in terms of sensitivity, which can be explained by high concentration and long pre-incubation time in fibril preparation. In these conditions, aggregation proceed to saturation, and large insulin fibers were expected to be formed. Based on these results, ThT detection prefers larger aggregate size over the FRET-Probe. As found earlier (Fig. 2C), shorter lag time was measured with the FRET-Probe over ThT, which indicate that the FRET-Probe can visualize also the formation of smaller and less mature fibers.

To study less mature fibrils further, we prepared 50 μM insulin solution with pre-incubation at 60 °C for 8 h. The condition was selected based on the earlier results as both methods had reached saturation after 8 h (Fig. 2A). The pre-incubated solutions were diluted and titrated from 0.004 to 4.54 μM with FRET-Probe and ThT (Fig. 3B). We set the S/B ratio of 2 as the cut-off value for insulin fibril detection, and obtained 10 nM and 148 nM insulin sensitivities for the FRET-Probe and ThT, respectively (Fig. 3B). This translates to 15-fold increase in sensitivity between FRET-Probe and ThT. These findings suggest that the FRET-Probe exhibits significantly greater sensitivity than ThT in detecting non-mature insulin fibers pre-incubated for 8 h. However, no significant difference is observed between the two probes for mature fibers pre-incubated for 28 h (Fig. 3A).

3.5. Effects of sodium salts to insulin fiber formation

The presence of NaCl has been shown to significantly promote insulin fiber formation [39,40] while Na_2SO_4 delays insulin aggregation by stabilizing the protein structure [41]. Additionally, it has been demonstrated that heating of insulin from 25 to 90 °C in the absence of NaCl does not result in an increase in ThT signal [39], suggesting that electrostatic repulsion between charged residues on the protein surface might prevent fibrillation under salt-free conditions [42]. Amyloid fibrils are also known to exhibit polymorphism depending on the presence of ions [43]. Thus, understanding of the FRET-Probe functionality in a changing aggregation condition is essential in our way to study for example commercial insulin formulations.

To investigate the effect of sodium salts, we conducted a study using 100 mM NaCl as a control, and compared the condition to 100 mM Na_2SO_4. With 50 μM insulin solutions incubated at 60 °C, the effect of NaCl and Na_2SO_4 on insulin aggregation rate was clear, as detected with the FRET-Probe and ThT assays (Fig. S6). As expected, NaCl was found to accelerate and Na_2SO_4 inhibit the insulin aggregation. Na_2SO_4 also inhibited the aggregation in the presence of NaCl, showing no significant difference compared to Na_2SO_4 alone. The most significant difference between the FRET-Probe and ThT was observed in the absence of sodium salt. The sigmoidal curve shape was similar with and without NaCl using the FRET-Probe, but ThT exhibited a less pronounced growth (Fig. S4). This suggests that the FRET-Probe might be more sensitive to detect distinct fibril polymorphs than ThT. Na_2SO_4 had small interfering effect on ThT measurements, as indicated by an elevated baseline signal (Fig. S6B). Collectively, these data affirm that the FRET-Probe is applicable in the presence of sodium salts that accelerate or inhibit insulin aggregation, and the data is comparable to ThT.

3.6. Detecting aggregation under neutral pH

It has been previously reported that insulin aggregates are not formed at 50–60 °C under neutral pH conditions without agitation, and the combination of heating and agitation is often required [17,28,34,44,

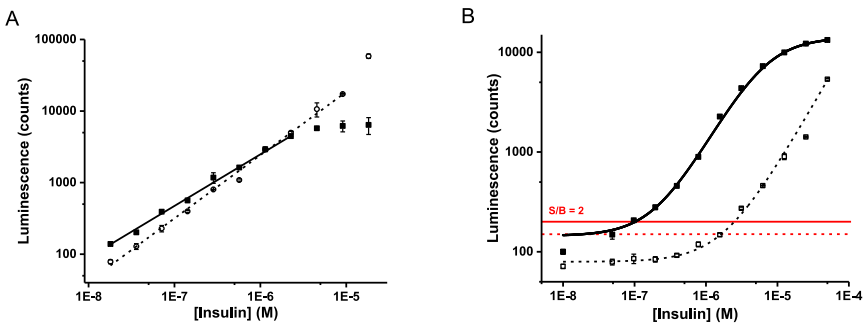

Fig. 3. Sensitivity of the insulin aggregation detection with the FRET-Probe and ThT. Titration of the pre-aggregated samples prepared using (**A**) 28 h incubation at 60 °C for 200 μM insulin and (**B**) 8 h incubation at 60 °C for 50 μM insulin, detected with the FRET-Probe (1 nM, solid line) and ThT (3 μM, dashed line). Data are presented as the mean ± SD (n = 3).

45]. Studying insulin under neutral conditions is important, as distinct features such as size, morphology, and structural organization are dependent on pH [45]. Thus, the FRET-Probe was investigated for the detectability of insulin aggregation under neutral pH and, moreover, aggregate structural variations.

First, we evaluated the FRET-Probe using 5–50 μM insulin samples in 20 mM HEPES (pH 7.5) containing 100 mM NaCl collected before and after agitation (shaking at 1250 rpm) at room temperature (RT). We found, that the TR-FRET signal exhibited a significant 20-fold increase for agitated samples after 20 h of incubation, providing the first evidence that the FRET-Probe is functional also for fibers formed under neutral pH conditions (Fig. S7). These first results were obtained using the previously optimized probe concentration. Optimizing probe concentrations revealed opposite trends for the FRET-Probe and ThT (Fig. S8). The FRET-Probe had greatest S/B at 0.5 nM, while ThT showed the highest S/B at 6.3 μM. Compared to acidic conditions, the optimal FRET-Probe concentration was halved, while for ThT it was doubled (Fig. S4, Fig. S8).

It is known that insulin concentration and aggregation rate are correlated in acidic solutions (Fig. 2) [34,37,38] as insulin oligomers act as on-pathway intermediates promoting fibril formation. However, the conflicting data exists on insulin aggregation in neutral pH solutions, with both inverse and direct correlations reported [34,44], however the experimental conditions were slightly different. Noormägi et al. [44] observed an inverse correlation at insulin concentrations of 2.5–30 μM, whereas Mawhinney et al. [34] reported a direct correlation at 2.5–30 μM but an inverse correlation at 50–100 μM. This difference might be due to the distinct mechanisms governing aggregation at neutral pH, as formed insulin oligomers can act as off-pathway species that compete with mature fibril formation. Thus, at higher concentrations the increased oligomer population reduces the monomeric insulins, thereby slowing fibrillation. This may not be the case at lower concentration, where monomers are more dominant. In addition, electrostatic repulsion between charged residues at neutral pH may promote kinetic barriers, requiring agitation to induce fibrillation.

Therefore, we investigated the aggregation rate of 5–50 μM insulin incubated in 20 mM HEPES (pH 7.5) at 50 °C with slow agitation (300 rpm). Samples were collected at designated intervals and monitored simultaneously using the FRET-Probe (0.5 nM) and ThT (6.3 μM) (Fig. S9). All samples were detectable with both the FRET-Probe and ThT; however, the FRET-Probe demonstrated a higher S/B ratio and shorter lag times across all samples (Fig. S9). Interestingly, unlike in acidic conditions, no clear direct or inverse correlation was observed between insulin concentration and aggregation rate in neutral pH. Insulin samples at 25 and 50 μM aggregated at a similar, faster rate compared to those at 5 and 10 μM, which exhibited comparable, slower aggregation.

3.7. Monitoring aggregation of insulin analogs

Therapeutic insulins are stored in their designated formulation to ensure the correct functionality. The formulation varies based on their structural and functional demand, as there are several different engineered insulins in the market. Insulin analogs constitute 42 % of all insulin sales and these are developed to provide slow and fast acting options for healthcare [10,11]. From these commercial options, we selected four distinct insulin formulations; Actrapid®, Fiasp® (aspart), Apidra® (glulisine), and Lantus® (glargine). Actarapid is a regular-acting recombinant human insulin, the same used in all previous assays, but in its designated buffer. Fiasp (aspart insulin) and Apidra (glulisine) are both considered fast-acting insulin analogs, and having single or double mutation in their B-chain, respectively [9,10]. Lantus (glargine) is a slow-acting analog, it has modifications both in the A- and B-chains [12]. The formulation of the commercial products is highly similar regarding insulin concentration (approximately 600 μM), the use of water for injections, HCl/NaOH for pH adjustment, and phenolic compounds for insulin stability (Table S2). However, there is also differences, from which the most relevant is the absence of zinc in Apidra (Table S2).

We first tested the commercial insulins by using incubation at 50 °C with agitation at 300 rpm. The condition is the same as previously with human insulin in neutral condition, and thus human insulin in H_2O was the control (Fig. S9). However, in this experiment the insulin concentration was significantly higher (~600 μM), as the commercial insulins were directly used in aggregation. With the FRET-Probe (0.5 nM) and ThT (6.3 μM) the same time-dependent pattern was visible using the both methods (Fig. 4). In all cases, the FRET-Probe detected insulin aggregation more rapidly than ThT, as expected. When we compared two fast-acting insulins, Fiasp and Apidra, we found that Apidra aggregated slightly faster than Fiasp (Fig. 4A). When the human insulin in H_2O was compared with the regular-acting Actrapid and slow-acting Lantus, we interestingly observed that Lantus and insulin in H_2O showed similar aggregation tendency, as the rate with Actrapid was significantly slower (Fig. 4B).

As zinc is added into insulin formulations to stabilize the hexamer form, we next investigated the impact of zinc on Actrapid and human insulin without formulation (H_2O). With the latter, both addition and removal increased the aggregation rate (Fig. 5A). When zinc was chelated with EDTA (600 μM) to produce zinc-free insulin, the results with the FRET-Probe and ThT are in line. However, when 150 μM zinc was added, creating an insulin-to-zinc ratio of 2:1, the aggregation rate increased significantly when detected by the FRET-Probe (Fig. 5A). Previous studies have shown that a 1:3 insulin-to-zinc ratio reduces aggregation compared to zinc-free insulin [46], while 3:1 and 1:6 ratios accelerate aggregation [47]. These results demonstrate the importance of the zinc concentration for insulin stability. When the zinc chelation was performed for Actrapid, a clear increase in aggregation rate was observed with both methods (Fig. 5B). However, even in the presence of EDTA, Actrapid exhibited a slower aggregation rate compared to zinc-free human insulin in H_2O. This difference may result from incomplete zinc chelation or the presence of additives, such as phenolic compounds, which can stabilize insulin into less accessible R_6 conformation, as discussed later (see Section 3.7.).

The increase in insulin aggregation upon zinc removal can be explained by hexameric insulin dissociation, but the mechanism behind the increased aggregation rate with higher zinc concentrations is unclear. Additionally, the clear difference between the FRET-Probe and ThT results in the presence of added zinc raises questions about the aggregation mechanism (Fig. 5A). It has been shown that zinc-free insulin primarily aggregates through second-order diffusion-limited aggregation (isodesmic aggregation), while zinc-insulin hexamers follow a nucleation-and-growth mechanism [47]. These distinct aggregation pathways are likely to produce aggregates with differing structures or morphologies, which might suggest that the FRET-Probe is more sensitive to early nucleation events or specific interactions within hexamers, while ThT preferentially detect fibrillar aggregates associated with isodesmic growth.

3.8. Monitoring of insulin hexameric forms

Insulin hexamer undergoes a TR transition, meaning it exists in equilibrium in three conformational states: T_6, $T_3R_3^f$, and R_6. When insulin and zinc concentrations are sufficient, insulin assembles into a T_6 hexamer consisting of three insulin dimers arranged around a threefold symmetry axis. The His^{B10} residues of each dimer coordinate a central zinc ion and the structure is stabilized by extended *N*-terminal B-chain residues (B1–B8), which cross between dimers and bury non-polar residues in adjacent dimers [48]. The T_6 conformation is recognized as an active monomeric structure [1]. In contrast, the R structure differs from the T by adopting a helical arrangement in the first eight amino acids of the B-chain (B1–B8) [49]. This structural change significantly alters the position of the *N*-terminal residues and enables the formation of a

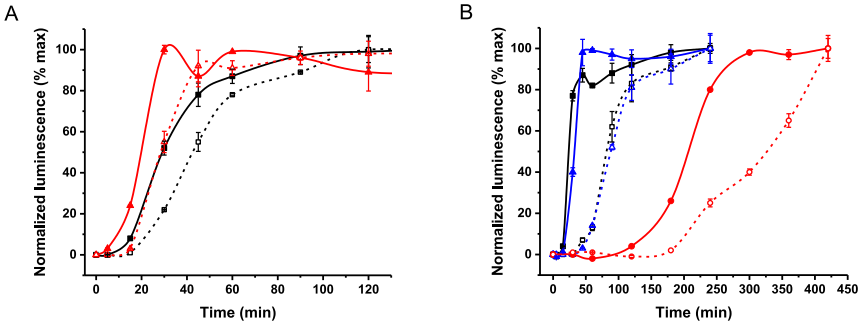

Fig. 4. Aggregation rates of different insulins in their commercial formulations. The FRET-Probe (solid line) and ThT (dashed line) detection of 600 μM (**A**) Fiasp (black) and Apidra (red) or (**B**) Lantus (black), Actrapid (red), and human insulin (blue) in H_2O. Samples were prepared using 50 °C incubation with agitation at 300 rpm. All commercial insulins were used in their own commercial formulations. Data are presented as the mean ± SD (n = 3). (For interpretation of the references to colour in this figure legend, the reader is referred to the Web version of this article.)

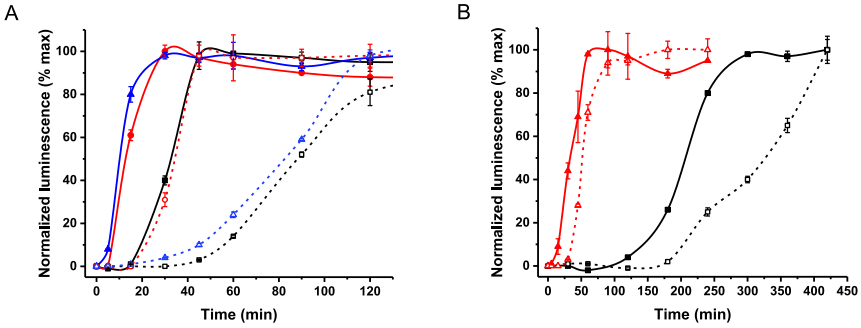

Fig. 5. The effect of zinc on insulin aggregation rate. (**A**) Aggregation of 600 μM human insulin in H_2O was studied in the absence (black) and presence of 150 μM $ZnCl_2$ (blue) or 600 μM EDTA (red) using the FRET-Probe (solid line) and ThT (dashed line). (**B**) Actrapid insulin aggregation was studied in the absence (red) and presence (black) of 600 μM EDTA using the FRET-Probe (solid line) and ThT (dashed line) for detection. Samples were prepared at 50 °C using agitation at 300 rpm. Data are presented as the mean ± SD (n = 3). (For interpretation of the references to colour in this figure legend, the reader is referred to the Web version of this article.)

secondary zinc coordination site including His^{B5} and His^{B10}. In the R_6 form, all six subunits adopt this helical B1–B8 structure, and it is known that phenolic compounds, such as phenol, resorcinol, and *m*-cresol, stabilize the R_6 conformation through hydrogen bonding and van der Waals interactions between dimers. In the presence of anionic ligands, TR transition occurs in only three monomers. The R conformation induced by anionic ligands differs from that stabilized by phenolic compounds by extending the three first amino acids on the B-chain, creating a $T_3R_3^f$ hexamer [7]. In pharmaceutical insulin analogs, phenolic compounds are added not only for their antibacterial properties (*m*-cresol), but also for their ability to induce the TR transition [8]. This area of research is highly important as novel insulin analogs are constantly engineered, and the same outcome can be achieved with varying means. As an example, fast-acting aspart is predominantly in the T_3R_3 conformation, while the another fast-acting insulin (glulisine) in the zinc-free T_6 conformation [50,51].

During the aggregation studies with the FRET-Probe, we detected unexpected results when some of the compounds commonly used in commercial insulins were studied individually. Under the acidic conditions, insulin aggregates were formed at pH 1.8, and measurements were conducted using a detection solution at pH 7.5. The aggregate-to-detection volume ratio was 1:11, resulting in a final pH of approximately 5. Under neutral conditions, the setup was reversed: aggregates were formed at pH 7.5, while the detection solution had a pH of 4, also yielding a final pH of around 5. However, when we used the same detection solution as in the acidic conditions to analyze aggregates formed at neutral pH, we observed an increase in signal even before aggregation occurred.

To explore whether the FRET-Probe could monitor conformational shifts in insulin hexamers, we supplemented 600 μM insulin with 150 μM $ZnCl_2$ to induce the T_6 hexamer. Then we performed a resorcinol titration to induce the TR transition in the presence or absence of common anionic compounds: 50 mM KSCN and 200 mM NaCl (Fig. 6A). In resorcinol-free insulin solutions, the TR-FRET signal remained high, independent of KSCN or NaCl. However, both KSCN and NaCl reduced the signal intensity. When resorcinol was titrated, the TR-FRET signal decreased at significantly lower concentrations in the presence of KSCN and NaCl (EC_{50}: 11 mM and 18 mM, respectively) compared to their absence (EC_{50}: 62 mM) (Fig. 6A). These results suggest that the FRET-Probe is sensitive to insulin conformational changes, distinguishing between different hexameric forms.

To test the hypothesis that the FRET-Probe preferentially binds to the T_6 hexamer and to a lesser extent to $T_3R_3^f$ and R_6 hexamers, we conducted a stepwise assay using 30 μM human insulin (Fig. 6B). Unlike previous assays, the FRET-Probe was added at the beginning of the reaction, and $Zn(ClO_4)_2$ was used instead of $ZnCl_2$. The result indicates, that the insulin alone is mostly present in dimer, and converted to T_6 upon zinc addition. Further addition of KSCN turns insulin in $T_3R_3^f$, and further to R_6 upon resorcinol addition to same wells. It is expected that the change in equilibrium rather than full TR transition is monitored with the FRET-Probe. However, by providing real-time monitoring of conformational transitions, the FRET-Probe can provide useful information on analog action profile engineering, not possible with other simple to use luminescent methodologies. Detecting shifts in hexameric

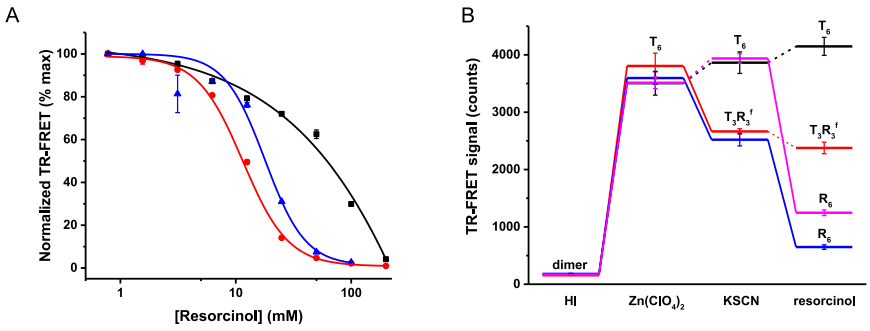

Fig. 6. The FRET-Probe based insulin hexamer detection. (**A**) Resorcinol titration (0.78–200 mM) with 600 μM human insulin supplemented with 150 μM $ZnCl_2$ and in the absence (black) and presence of 50 mM KSCN (red) and 200 mM NaCl (blue) mixed with FRET-Probe. (**B**) Real-time monitoring of 30 μM human insulin TR transition using in a stepwise assay using 12 μM $Zn(ClO_4)_2$, 5 mM KSCN and 5 mM resorcinol. TR-FRET signal is monitored after 10 min incubation at each step. The names on top of the signal bars indicate the presumed dominating insulin form in the solution. Solid lines between vertical signal bars indicate addition, while dashed lines indicate controls without addition. Data is presented as the mean ± SD (n = 3). HI = human insulin. (For interpretation of the references to colour in this figure legend, the reader is referred to the Web version of this article.)

equilibrium can also guide modifications to enhance thermal and chemical stability, critical for storage and therapeutic efficacy.

4. Conclusions

In this study, we demonstrate the potential of the FRET-Probe technique for studying insulin aggregation and changes in hexameric conformations. In the insulin aggregation assays, the FRET-Probe showed high specificity and sensitivity, distinguishing insulin fibrils from native insulin and consistently exhibiting shorter lag times and higher signal-to-background (S/B) ratios compared to the standard ThT assay (Table S1). The FRET-Probe assay implementation and throughput are as simple as with the ThT and other dyes, but the higher sensitivity and earlier detection makes it tempting option for *in vitro* setting. Results indicate that the FRET-Probe detects aggregates that might distinct fibrillar morphology, but that it can be used also for other amyloid fibril forming peptides than insulin. The FRET-Probe ability to provide early insights into insulin fibril formation holds promise for advancing our understanding of amyloid-related diseases and improving therapeutic interventions. This study contributes to the refinement of techniques for amyloid fibril detection and offers valuable insights into the kinetics and mechanisms underlying insulin aggregation. Enhanced sensitivity with the FRET-Probe also might unravel the dynamics of insulin fibril formation, especially for early detection of amyloid fibrils, even its use for *in vivo* applications has not been studied.

The unique aspect of this work is the FRET-Probe ability to differentiate between insulin hexameric conformations (T_6, $T_3R_3^f$, and R_6), never shown with other probes. These transitions, are influenced by zinc ions, anionic ligands, and phenolic compounds, and were clearly detected using the FRET-Probe. The distinct signal profiles observed for each conformation highlight the FRET-Probe capability to resolve subtle structural dynamics within insulin hexamers in real-time. This feature offers a novel approach to studying the structural and functional properties of insulin formulations under various conditions, providing insights not attainable with existing detection methods.

CRediT authorship contribution statement

Morteza Malakoutikhah: Writing – original draft, Validation, Methodology, Investigation, Formal analysis, Conceptualization. **Laura Kauppi:** Writing – original draft, Validation, Investigation, Formal analysis. **Kalle Mäntylä:** Validation, Investigation. **Harri Härmä:** Writing – review & editing, Supervision, Methodology, Conceptualization. **Kari Kopra:** Writing – review & editing, Supervision, Resources, Methodology, Conceptualization.

Funding sources

This work was supported by the Research Council of Finland (323433/K.K. and 353324/K·K.).

Declaration of competing interest

The authors declare the following financial interests/personal relationships which may be considered as potential competing interests: Kari Kopra reports financial support was provided by Research Council of Finland. The authors declare the following competing financial interest(s): Harri Härmä have commercial interest through QRET Technologies. If there are other authors, they declare that they have no known competing financial interests or personal relationships that could have appeared to influence the work reported in this paper.

Acknowledgements

TEM imaging performed in the Laboratory of Electron Microscopy, Institute of Biomedicine, University of Turku, which receives financial support from Biocenter Finland.

Appendix. ASupplementary data

Supplementary data to this article can be found online at https://doi.org/10.1016/j.aca.2025.344366.

Data availability

Data will be made available on request.

References

[1] M. Lawrence, Understanding insulin and its receptor from their three-dimensional structures, Mol. Metabol. 52 (2021) 101255, https://doi.org/10.1016/j.molmet.2021.101255.
[2] M. Atkinson, et al., Type 1 diabetes, Lancet 383 (2014) 69–82, https://doi.org/10.1016/S0140-6736(13)60591-7.
[3] S. Chatterjee, et al., Type 2 diabetes, Lancet 389 (2017) 2239–2251, https://doi.org/10.1016/S0140-6736(17)30058-2.
[4] B. Zhou, et al., Worldwide trends in diabetes prevalence and treatment from 1990 to 2022: a pooled analysis of 1108 population-representative studies with 141 million participants, Lancet 404 (2024) 2077–2093, https://doi.org/10.1016/S0140-6736(24)02317-1.
[5] G. Lisi, C. Png, D. Wilcox, Thermodynamic contributions to the stability of the insulin hexamer, Biochemistry 53 (2014) 3576–3584, https://doi.org/10.1021/bi401678n.
[6] S. Rahuel-Clermont, C.A. French, N.C. Kaarsholm, M.F. Dunn, Mechanisms of stabilization of the insulin hexamer through allosteric ligand interactions, Biochemistry 36 (1997) 5837–5845, https://doi.org/10.1021/bi963038q.

[7] G.D. Smith, E. Ciszak, W. Pangborn, A novel complex of a phenolic derivative with insulin: structural features related to the T–R transition, Protein Sci. 5 (1996) 1502–1511, https://doi.org/10.1002/pro.5560050806.

[8] H. Berchtold, R. Hilgefeld, Binding of phenol to R_6 insulin hexamer, Biopolymers 51 (1999) 165–172, https://doi.org/10.1002/(SICI)1097-0282(1999)51:2<165::AID-BIP6>3.0.CO, 2-X.

[9] K.L. Simpson, C.M. Spencer, Insulin aspart, Drugs 57 (1999) 759–765, https://doi.org/10.2165/00003495-199957050-00013.

[10] D.M. Robinson, K. Wellington, Insulin glulisine, Drugs 66 (2006) 861–869, https://doi.org/10.2165/00003495-200666060-00011.

[11] J.L. Mann, et al., An ultrafast insulin formulation enabled by high-throughput screening of engineered polymeric excipients, Sci. Transl. Med. 12 (2020) eaba6676, https://doi.org/10.1126/scitranslmed.aba6676.

[12] G.B. Bolli, D.R. Owens, Insulin glargine, Lancet 356 (2000) 443–445, https://doi.org/10.1016/S0140-6736(00)02546-0.

[13] Y. Shikama, et al., Localized amyloidosis at the site of repeated insulin injection in a diabetic patient, Intern. Med. 49 (2010) 397–401, https://doi.org/10.2169/internalmedicine.49.2633.

[14] T. Nagase, et al., Insulin-derived amyloidosis and poor glycemic control: a case series, Am. J. Med. 127 (2014) 450–454, https://doi.org/10.1016/j.amjmed.2013.10.029.

[15] J. Haas, E. Vöhringer-Martinez, A. Bögehold, et al., Primary steps of pH-Dependent insulin aggregation kinetics are governed by conformational flexibility, Chembiochem 10 (2009) 1816–1822, https://doi.org/10.1002/cbic.200900266.

[16] S. Haghighi-Poodeh, B. Kurganov, L. Navidpour, P. Yaghmaei, A. Ebrahim-Habibi, Characterization of arginine preventive effect on heat-induced aggregation of insulin, Int. J. Biol. Macromol. 145 (2020) 1039–1048, https://doi.org/10.1016/j.ijbiomac.2019.09.196.

[17] R. Malik, I. Roy, Probing the mechanism of insulin aggregation during agitation, Int. J. Pharm. 413 (2011) 73–80, https://doi.org/10.1016/j.ijpharm.2011.04.024.

[18] L. Nault, et al., Human insulin adsorption kinetics, conformational changes and amyloidal aggregate formation on hydrophobic surfaces, Acta Biomater. 9 (2013) 5070–5079, https://doi.org/10.1016/j.actbio.2012.09.025.

[19] C. Zhou, W. Qi, E.N. Lewis, J.F. Carpenter, Characterization of sizes of aggregates of insulin analogs and the conformations of the constituent protein molecules: a concomitant dynamic light scattering and raman spectroscopy study, J. Pharmaceut. Sci. 105 (2016) 551–558, https://doi.org/10.1016/j.xphs.2015.10.023.

[20] J.L. Jiménez, et al., The protofilament structure of insulin amyloid fibrils, Proc. Natl. Acad. Sci. USA. 99 (2002) 9196–9201, https://doi.org/10.1073/pnas.142459399.

[21] L. Wang, et al., Structural basis of insulin fibrillation, Sci. Adv. 9 (2023) eadi1057, https://doi.org/10.1126/sciadv.adi1057.

[22] S. Suladze, et al., Atomic resolution structure of full-length human insulin fibrils, Proc. Natl. Acad. Sci. USA. 121 (2024) e2401458121, https://doi.org/10.1073/pnas.2401458121.

[23] W. Dzwolak, v. Smirnovas, R. Jansen, R. Winter, Insulin forms amyloid in a strain-dependent manner: an FT-IR spectroscopic study, Protein Sci. 13 (2004) 1927–1932, https://doi.org/10.1110/ps.03607204.

[24] R. Coppolino, S. Coppolino, V. Villari, Study of the aggregation of insulin glargine by light scattering, J. Pharmaceut. Sci. 59 (2006) 1029–1034, https://doi.org/10.1002/jps.20609.

[25] E. Pryor, J.A. Kotarek, M.A. Moss, C.N. Hestekin, Monitoring insulin aggregation via capillary electrophoresis, Int. J. Mol. Sci. 12 (2011) 9369–9388, https://doi.org/10.3390/ijms12129369.

[26] Y. Kim, J.E. Shields, pH dependent conformational changes in the T-and R-states of insulin in solution: circular dichroic studies in the pH range of 6 to 10, Biochem. Biophys. Res. Commun. 186 (1992) 1115–1120, https://doi.org/10.1016/0006-291X(92)90862-F.

[27] M. Biancalana, K. Makabe, A. Koide, S. Koide, Molecular mechanism of Thioflavin-T binding to the surface of β-Rich peptide self-assemblies, J. Mol. Biol. 384 (2009) 1052–1063, https://doi.org/10.1016/j.jmb.2008.11.006.

[28] M.I. Sulatsky, et al., Effect of the fluorescent probes ThT and ANS on the mature amyloid fibrils, Prion 14 (2020) 67–75, https://doi.org/10.1080/19336896.2020.1720487.

[29] R. Mishra, D. Sjölander, P. Hammarström, Spectroscopic characterization of diverse amyloid fibrils in vitro by the fluorescent dye nile red, Mol. Biosyst. 7 (2011) 1232–1240, https://doi.org/10.1039/c0mb00236d.

[30] R. Mahran, et al., Isothermal chemical denaturation assay for monitoring protein stability and inhibitor interactions, Sci. Rep. 13 (2023) 20066, https://doi.org/10.1038/s41598-023-46720-w.

[31] T. Sneideris, et al., pH-Driven polymorphism of insulin amyloid-like fibrils, PLoS One 10 (2015) e0136602, https://doi.org/10.1371/journal.pone.0136602.

[32] M. Ishigaki, K. Morimoto, E. Chatani, Y. Ozaki, Exploration of insulin amyloid polymorphism using raman spectroscopy and imaging, Biophys. J. 118 (2020) 2997–3007, https://doi.org/10.1016/j.bpj.2020.04.031.

[33] S. Jha, et al., pH dependence of amylin fibrillization, Biochemistry (Mosc.) 53 (2014) 300–310, https://doi.org/10.1021/bi401164k.

[34] M.T. Mawhinney, T.L. Williams, J.L. Hart, M.L. Taheri, B. Urbanc, Elucidation of insulin assembly at acidic and neutral pH: characterization of low molecular weight oligomers, Proteins: Struct., Funct., Bioinf. 55 (2017) 2096–2110, https://doi.org/10.1002/prot.25365.

[35] R. Kumar, A. Nordberg, T. Darreh-Shori, Amyloid-β peptides act as allosteric modulators of cholinergic signalling through formation of soluble BAβACs, Brain 139 (2016) 174–192, https://doi.org/10.1093/brain/awv318.

[36] C. Xue, T.Y. Lin, D. Chang, Z. Guo, Thioflavin T as an amyloid dye: fibril quantification, optimal concentration and effect on aggregation, R. Soc. Open Sci. 4 (2017) 160696, https://doi.org/10.1098/rsos.160696.

[37] L. Nielsen, et al., Effect of environmental factors on the kinetics of insulin fibril formation: elucidation of the molecular mechanism, Biochemistry 40 (2001) 6036–6046, https://doi.org/10.1021/bi002555c.

[38] R. Morris, et al., Mechanistic and environmental control of the prevalence and lifetime of amyloid oligomers, Nat. Commun. 4 (2013) 1891, https://doi.org/10.1038/ncomms2909.

[39] E. Chatani, H. Imamura, N. Yamamoto, M. Kato, Stepwise organization of the β-structure identifies key regions essential for the propagation and cytotoxicity of insulin amyloid fibrils, J. Biol. Chem. 289 (2014) 10399–10410, https://doi.org/10.1074/jbc.M113.520874.

[40] M. Muzaffar, A. Ahmad, The mechanism of enhanced insulin amyloid fibril formation by NaCl is better explained by a conformational change model, PLoS One 6 (2011) e27906, https://doi.org/10.1371/journal.pone.0027906.

[41] M. Owczarz, P. Arosio, Sulfate anion delays the self-assembly of human insulin by modifying the aggregation pathway, Biophys. J. 107 (2014) 197–207, https://doi.org/10.1016/j.bpj.2014.05.030.

[42] K. Klement, et al., Effect of different salt ions on the propensity of aggregation and on the structure of alzheimer's Aβ(1-40) amyloid fibrils, J. Mol. Biol. 373 (2007) 1321–1333, https://doi.org/10.1016/j.jmb.2007.08.068.

[43] T. Hiramatsu, et al., Iodine staining as a useful probe for distinguishing insulin amyloid polymorphs, Sci. Rep. 10 (2020) 16741, https://doi.org/10.1038/s41598-020-73460-y.

[44] A. Noormägi, J. Gavrilova, J. Smirnova, V. Tõugu, P. Palumaa, Zn(II) ions co-secreted with insulin suppress inherent amyloidogenic properties of monomeric insulin, Biochem. J. 430 (2010) 511–518, https://doi.org/10.1042/BJ20100627.

[45] C. Iannuzzi, M. Borriello, M. Portaccio, G. Irace, I. Sirangelo, Insights into insulin fibril assembly at physiological and acidic pH and related amyloid intrinsic fluorescence, Int. J. Mol. Sci. 18 (2017) 2551, https://doi.org/10.3390/ijms18122551.

[46] C. Frankær, et al., Insulin fibrillation: the influence and coordination of Zn2+, J. Stuct. Biol. 199 (2017) 27–38, https://doi.org/10.1016/j.jsb.2017.05.006.

[47] Y. Xu, Y. Yan, D. Seeman, L. Sun, P.L. Dubin, Langmuir 28 (2012) 579–586, https://doi.org/10.1021/la202902a.

[48] G.D. Smith, W.A. Pangborn, R.H. Blessing, The structure of T6 human insulin at 1.0Å resolution, Acta Crystallogr. D 59 (2003) 474–482, https://doi.org/10.1107/S0907444902023685.

[49] S.I. O'Donoghue, et al., Unraveling the symmetry ambiguity in a hexamer: calculation of the R6 human insulin structure, J. Biomol. NMR 16 (2000) 93–108, https://doi.org/10.1023/A:1008323819099.

[50] L. Palmieri, M. Fávero-Retto, D. Lourenço, L. Mauricio, T.R. Lima, A T3R3 hexamer of the human insulin variant B28Asp, Biophys. Chem. 173 (2013) 1–7, https://doi.org/10.1016/j.bpc.2013.01.003.

[51] R.B. Gillis, et al., Analysis of insulin glulisine at the molecular level by X-ray crystallography and biophysical techniques, Sci. Rep. 11 (2021) 1737, https://doi.org/10.1038/s41598-021-81251-2.